A LETTERS JOURNAL EXPLORING THE FRONTIERS OF PHYSICS

OFFPRINT

Structural, electronic and mechanical properties of Imma-carbon

QUN WEI, MEIGUANG ZHANG, HAIYAN YAN, ZHENGZHE LIN and XUANMIN ZHU

EPL, **107** (2014) 27007

epl

A Letters Journal Exploring the Frontiers of Physics

AN INVITATION TO SUBMIT YOUR WORK

www.epljournal.org

The Editorial Board invites you to submit your letters to EPL

EPL is a leading international journal publishing original, high-quality Letters in all areas of physics, ranging from condensed matter topics and interdisciplinary research to astrophysics, geophysics, plasma and fusion sciences, including those with application potential.

The high profile of the journal combined with the excellent scientific quality of the articles continue to ensure EPL is an essential resource for its worldwide audience. EPL offers authors global visibility and a great opportunity to share their work with others across the whole of the physics community.

Run by active scientists, for scientists

EPL is reviewed by scientists for scientists, to serve and support the international scientific community. The Editorial Board is a team of active research scientists with an expert understanding of the needs of both authors and researchers.

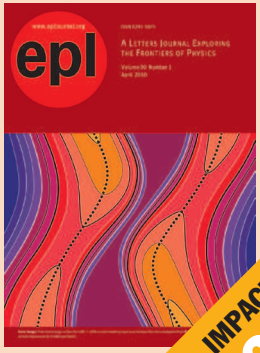

IMPACT FACTOR 2.753*

*As ranked by ISI 2010

IMPACT FACTOR
2.753*
* As listed in the ISI® 2010 Science Citation Index Journal Citation Reports

OVER
500 000
full text downloads in 2010

30 DAYS
average receipt to online publication in 2010

16 961
citations in 2010
37% increase from 2007

"We've had a very positive experience with EPL, and not only on this occasion. The fact that one can identify an appropriate editor, and the editor is an active scientist in the field, makes a huge difference."

Dr. Ivar Martinv
Los Alamos National Laboratory, USA

Six good reasons to publish with EPL

We want to work with you to help gain recognition for your high-quality work through worldwide visibility and high citations.

1. **Quality** – The 40+ Co-Editors, who are experts in their fields, oversee the entire peer-review process, from selection of the referees to making all final acceptance decisions
2. **Impact Factor** – The 2010 Impact Factor is 2.753; your work will be in the right place to be cited by your peers
3. **Speed of processing** – We aim to provide you with a quick and efficient service; the median time from acceptance to online publication is 30 days
4. **High visibility** – All articles are free to read for 30 days from online publication date
5. **International reach** – Over 2,000 institutions have access to EPL, enabling your work to be read by your peers in 100 countries
6. **Open Access** – Articles are offered open access for a one-off author payment

Details on preparing, submitting and tracking the progress of your manuscript from submission to acceptance are available on the EPL submission website **www.epletters.net**.

If you would like further information about our author service or EPL in general, please visit **www.epljournal.org** or e-mail us at **info@epljournal.org**.

EPL is published in partnership with:

European Physical Society | Società Italiana di Fisica | EDP Sciences | IOP Publishing

epl A Letters Journal Exploring the Frontiers of Physics

July 2014

EPL, **107** (2014) 27007
doi: 10.1209/0295-5075/107/27007

www.epljournal.org

Structural, electronic and mechanical properties of Imma-carbon

Qun Wei[1(a)], Meiguang Zhang[2(b)], Haiyan Yan[3], Zhengzhe Lin[1] and Xuanmin Zhu[1]

[1] *School of Physics and Optoelectronic Engineering, Xidian University - 710071 Xi'an, PRC*
[2] *Department of Physics and Information Technology, Baoji University of Arts and Sciences - 721016 Baoji, PRC*
[3] *College of Chemistry and Chemical Engineering, Baoji University of Arts and Sciences - 721013 Baoji, PRC*

received 17 April 2014; accepted in final form 29 June 2014
published online 15 July 2014

PACS 71.15.Mb – Density functional theory, local density approximation, gradient and other corrections
PACS 71.20.-b – Electron density of states and band structure of crystalline solids
PACS 62.20.de – Elastic moduli

Abstract – A theoretical investigation on mechanical and electronic properties of Imma-carbon was performed by employing first-principles calculations based on the density functional theory. The stability at ambient condition is approved by phonon dispersion and elastic constants calculations. The analysis of elastic anisotropy and hardness anisotropy shows that Imma-carbon is nearly mechanical isotropy. The large elastic constants and ideal strength indicate Imma-carbon is a potential superhard material. Ideal strength studies show that (010) plane is the easy cleavage plane for Imma-carbon, and the cleavage mechanism was discussed in detail. The calculated band structure is a direct band gap semiconductor with 2.97 eV gap at Γ-point.

Introduction. – Owing to its flexibility of bond hybridization, pure carbon can adopt various structures with vastly different properties, from the superhard insulating (diamond, lonsdaleite, and other hypothetical phases) to ultrasoft semimetallic (graphite, fullerenes), and even superconducting (doped diamond). At ambient conditions, it is known that graphite is the most stable phase of carbon where the atoms crystallize in hexagonal sp^2 planes bound together by weak van der Waals forces. Under high pressures and high temperatures (HPHT), other bulk allotropic metastable forms of superhard diamond and lonsdaleite (the carbon atoms are arranged in a sp^3 network) synthesized from graphite has had revolutionary impacts on modern society ranging from industrial applications, to technological advances in contemporary high-tech applications, and to scientific exploration of materials' behavior under extreme conditions. One important direction in carbon research is the discovery of carbon allotropes with advanced mechanical and electronic properties. Unlike the direct transition from graphite to diamond under simultaneously HPHT, several experiments reported that cold compression of graphite produces a metastable superhard and transparent phase. The nature of cold-compressed graphite has been resolved by Boulfelfel and Wang *et al.* [1,2] to be M-carbon.

In order to shed some light on the experimental structural uncertainties, sophisticated theoretical computational works have proposed a series of possible candidates to explain the experimental x-ray diffraction pattern, including monoclinic carbon phases (M-, F-, X-carbon) [3–5], orthorhombic phases (*e.g.*, C-, H-, R-, S-, W-, Z-, Z-ACA, Z-CACB, Z4-A3B1, A4-A2B2 and oC32-carbon) [5–9], cubic bct-C_4 phase [10], etc. These superhard sp^3 phases were mostly obtained through *ab initio* crystal prediction methods, where the energy landscape of carbon at high pressure is explored. Among these predicted structures, M-carbon was firstly proposed to be the candidate for the cold-compressed graphite, demonstrated by the x-ray diffraction patterns and energy barrier using molecular-dynamics transition path sampling simulations [3]. Furthermore, many of these phases have been characterized theoretically through the calculations of their electronic structure, optical and mechanical properties, IR spectra, Raman spectra, etc. Nevertheless, the crystal structure of cold-compressed graphite is still the subject of intense discussions in the literature. More recently, a superhard sp^3-hybridized crystalline carbon allotrope with orthorhombic Imma symmetry was reported by Zhang *et al.* [11] and this orthorhombic Imma

(a) E-mail: weiaqun@163.com
(b) E-mail: zhmgbj@126.com

Table 1: The calculated lattice parameters and bond lengths (in Å), EOS fitted bulk modulus B_0 (in GPa), and its derivative B_0' for Imma-carbon.

Method	a	b	c	$d_{\text{C1-C1}}$	$d_{\text{C2-C2}}$	$d_{\text{C1-C2}}$	B_0	B_0'
				1.5228	1.5431	1.5420		
GGA	7.5968	4.2841	4.3635	1.5619	1.5894		408	3.69
				1.5679				
GGA [11]	7.596	4.283	4.363					
				1.5062	1.5265	1.5251		
LDA	7.5157	4.2369	4.3177	1.5463	1.5699		440	3.62
				1.5529				

phase exhibits much energetically superior to some previously proposed cold-compressed carbon phases (F-carbon, M-carbon, bct-C_4, etc.). Compared to the detail physical properties reported in previous predicted carbon allotropes, the structure, mechanical and electronic properties of Imma-carbon remain large unexplored. In the present work, we have extended the mechanical properties and presented in detail the stress-strain relations upon tension and shear of Imma phase in order to investigate the intrinsic cleavage mechanism. Meanwhile, the calculated results of elastic and hardness anisotropy indicate that Imma-carbon can be regarded as an isotropy material at ambient pressure.

Computational details. – Our calculations were performed using the VASP code with the generalized gradient approximation (GGA) [12] and local density approximation (LDA) [13] for exchange correlation functional. The integration in the Brillouin zone was employed using the Monkhorst-Pack scheme ($8 \times 8 \times 8$) and the energy cutoff of 900 eV were chosen to ensure that energy calculations are converged to better than 1 meV/atom. The electron and core interactions were included by using the frozen-core all-electron projector augmented wave (PAW) method [14], with C:$2s^2 2p^2$ treated as the valence electrons. The elastic constants were determined from evaluation of stress tensor generated small strain. Bulk modulus, shear modulus, Young's modulus, and Poisson's ratio were estimated by using Voigt-Reuss-Hill approximation [15]. The stress-strain relationships were calculated by incrementally deforming the model cell in the direction of the applied strain, and simultaneously relaxing the cell basis vectors conjugated to the applied strain, as well as the positions of atoms inside the cell, at each step. To ensure that the strain path is continuous, the starting position at each strain step has been taken from the relaxed coordinates of the previous strain step.

Results and discussions. – The equilibrium structural parameters for Imma-carbon were obtained by full relaxations of both lattice constants and internal atomic coordination. As listed in table 1, the optimized lattice constants within LDA (GGA) level at ambient pressure

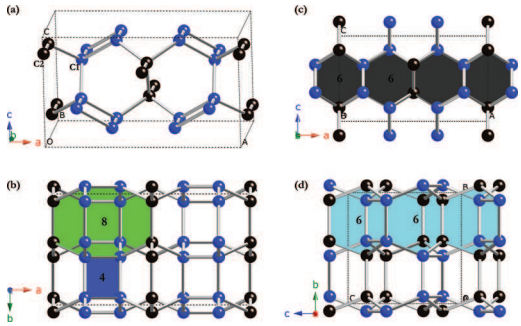

Fig. 1: (Colour on-line) Global view of Imma-carbon in a unit cell (a); view of Imma-carbon along the [001] direction (b); view of Imma-carbon along the [010] direction (c); view of Imma-carbon along the [100] direction (d). C1 atoms are denoted as blue spheres and C2 black.

are $a = 7.5157$ Å (7.5968 Å), $b = 4.2369$ Å (4.2841 Å) and $c = 4.3177$ Å (4.3635 Å) in a unit cell, in which two inequivalent carbon atoms C1 and C2 occupy the Wyckoff $16j$ (0.1605, 0.0667, 0.3383) and $8h$ (0.5, 0.0647, 0.6650) sites at LDA level, respectively. These structural parameters are in good agreement with the theoretical results predicted by Zhang *et al.* [11]. As shown in fig. 1(a), both C1 and C2 atoms are tetrahedrally bonded, and C1 atoms locate at the corner of a planar rectangle with the bond length of 1.5463 Å and 1.5529 Å. Moreover, the Imma-carbon exhibits distinct topologies featuring with even (4, 6, and 8) rings which are similar to those of oC16-II-carbon and Oc32-carbon. This Imma-carbon looks very similar to Y-carbon (space group Cmca) in ref. [5]. They both have $4+8$ topology. But in Y-carbon, C atoms only occupy one $16g$ site. In more detail, the four-coordinated carbon atoms form 4-membered and 8-membered rings on the (001) projection (fig. 1(b)). Along the [010] direction (fig. 1(c)), there are two types of 6-membered rings consisting of 4C1 atoms and 2C2 atoms. Other two types of 6-membered rings appear in the view along the [100] direction (as shown in fig. 1(d)), one consists of 2C1 atoms and 4C2 atoms, the other consists of 4C1 atoms and 2C2 atoms. At zero temperature, a stable crystalline structure requires all phonon frequencies to be

Table 2: The elastic constants C_{ij} (GPa), bulk modulus B (GPa), shear modulus G (GPa), Young's modulus E (GPa) and Poisson's ratio ν of Imma-carbon within LDA, compared with other superhard materials.

	C_{11}	C_{22}	C_{33}	C_{44}	C_{55}	C_{66}	C_{12}	C_{13}	C_{23}	G	E	ν
Diamond [17]	1104			599			149			550	1185	0.077
oC32 [17]	1195	1269	1259	477	552	408	54	111	31	522	1135	0.087
c-BN [17]	820			477			194			412	921	0.119
Imma-carbon	1126	1105	1196	446	526	377	86	121	61	476	1049	0.102

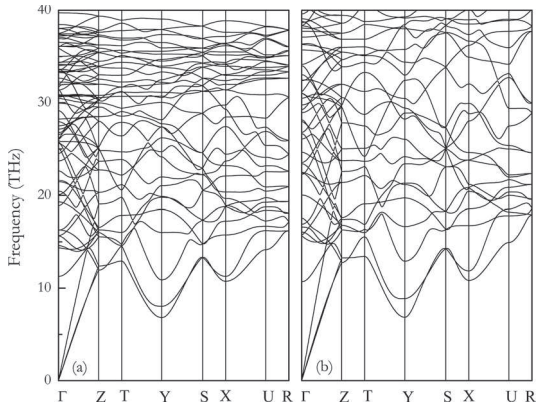

Fig. 2: Phonon dispersion of Imma-carbon at 0 GPa (a) and 100 GPa (b).

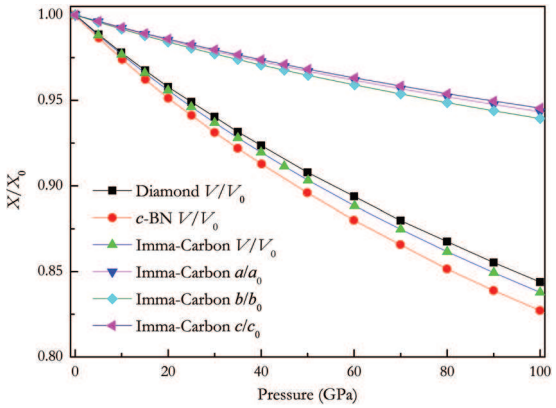

Fig. 3: (Colour on-line) Variation of ratio as a function of pressure.

positive. We have thus performed the calculations on the phonon dispersion curve of Imma-carbon at 0 GPa and 100 GPa, respectively. As shown in fig. 2, no imaginary phonon frequency was detected in the whole Brillouin zone for Imma-carbon, indicating its dynamical stability up to 100 GPa. The total energy of Imma-carbon was minimized as a function of the selected unit cell volume at different pressure. By fitting the E-V data at different pressures into the third-order Birch-Murnaghan equation of states (EOS) [16], we obtained the values of equilibrium bulk modulus and its pressure derivative for Imma-carbon are 440 GPa and 3.62 at LDA level. One can see that the bulk modulus of Imma-carbon can be comparable to that of c-BN (403 GPa) and other carbon polymorphs [17], *e.g.*, diamond (467 GPa), bct-C_4 (437 GPa), oC_{32}(457 GPa), Cco-C_8(449 GPa), C-carbon (444 GPa), M-carbon (434 GPa), and W-carbon (437 GPa). To further compare the incompressibility of Imma-carbon, c-BN and diamond under pressure, the volume compressions as a function of pressure are plotted in fig. 3. One can see that the incompressibility of Imma-carbon is less than that of diamond but larger than c-BN. This is in accordance with the previous results of bulk modulus. This indicates that Imma-carbon is an ultra-incompressible material.

To study the mechanical properties of Imma-carbon, the elastic constants are calculated by using the strain-stress method. The average bulk modulus, shear modulus and Young's modulus of the polycrystalline are further estimated by using the Voigt-Reuss-Hill approximation.

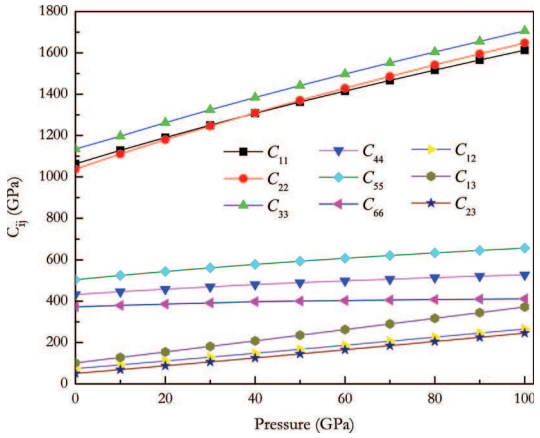

Fig. 4: (Colour on-line) Elastic constants of Imma-carbon as a function of pressure.

The obtained results are listed in table 2, together with the elastic parameters of diamond, c-BN, and oC32 for comparison. Firstly, it can be seen that the elastic constants of Imma-carbon obey the elastic stability criteria for an orthorhombic structure, and thus it can be mechanically stable under the ambient condition. Secondly, one can see that the shear modulus of Imma-carbon (476 GPa) is less than diamond (550) and oC32 (522 GPa) but larger than c-BN (412 GPa), indicating its strong resistance to shape change at a constant volume. The large Young's modulus of Imma-carbon (1049 GPa) comparable

Table 3: Calculated anisotropy factors A_1, A_2, A_3, A_{Ba}, A_{Bc}, A_G, A_B, directional bulk modulus B_a, B_b, B_c (in GPa) and the percentage anisotropy in compressibility and shear A_B, A_G (in %) of Imma-carbon.

Method	A_1	A_2	A_3	A_{Ba}	A_{Bc}	A_B	A_G
GGA	0.87	0.97	0.76	1.08	1.12	0.103	0.750
LDA	0.86	0.97	0.73	1.08	1.12	0.095	0.927

with diamond (1185 GPa) and oC32 (1135 GPa) shows its stiffness. To further illustrate the effect of pressure on the elastic properties of Imma-carbon, we exhibit the variations of elastic constants with pressure in fig. 4. As shown in fig. 4, nine independent elastic constants increase monotonically with pressure. Meanwhile, the predicted pressure derivatives of elastic constants, $\partial C_{11}/\partial P$, $\partial C_{22}/\partial P$, $\partial C_{33}/\partial P$ are found to be 5.53, 6.13 and 5.76, which are larger than those of other elastic constants. These results indicate that C_{11}, C_{33}, and C_{33} vary rapidly under the effect of pressure in comparison with the variations in other elastic constants. Furthermore, the calculated elastic constants under pressure up to 100 GPa also satisfy the well-known Born stability criteria, indicating that Imma-carbon under pressure is also mechanically stable.

The shear anisotropic factors provide a measure of the degree of anisotropy in the bonding between atoms in different planes. The shear anisotropic factor for the $\{100\}$ shear plane between the $\langle 011\rangle$ and $\langle 010\rangle$ directions is [18]

$$A_1 = \frac{4C_{44}}{C_{11} + C_{33} - 2C_{13}}. \tag{1}$$

For the $\{010\}$ shear planes between the $\langle 101\rangle$ and $\langle 001\rangle$ directions it is [18]

$$A_2 = \frac{4C_{55}}{C_{22} + C_{33} - 2C_{23}}, \tag{2}$$

and for the $\{001\}$ shear planes between the $\langle 110\rangle$ and $\langle 010\rangle$ directions it is [18]

$$A_3 = \frac{4C_{66}}{C_{11} + C_{22} - 2C_{12}}. \tag{3}$$

For an isotropic crystal, the shear anisotropy factors A_1, A_2, and A_3 must be 1.0. Any departure from 1.0 is a measure of the degree of elastic anisotropy. The calculated results for the Imma-carbon are shown in table 3. The anisotropy for the $\{001\}$ shear planes between the $\langle 110\rangle$ and $\langle 010\rangle$ directions is the largest. In addition, the bulk modulus along the a-, b- and c-axis are defined as $B_i = i(\mathrm{d}P/\mathrm{d}i)$ with $i = a$, b and c. Then the anisotropies of the bulk modulus along the a-axis and c-axis with respect to the b-axis can be expressed as $A_{Ba} = B_a/B_b$ and $A_{Bc} = B_c/B_b$. The calculated results are also listed in table 3. One can see that the directional bulk modulus along the a-axis and c-axis is slightly larger than that along the b-axis, which is in agreement with the pressure dependence of the normalized lattice parameters

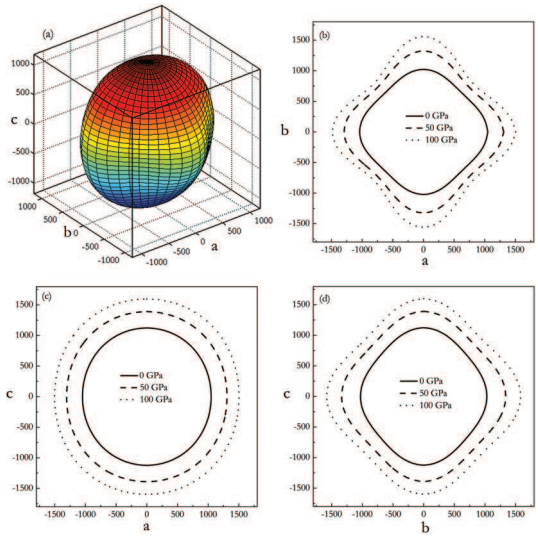

Fig. 5: (Colour on-line) Illustration of the directional dependent Young's modulus of the Imma-carbon (a), and the projections of the directional dependent Young's modulus in different plans: ab plane (b), ac plane (c), and bc plane (d).

(see fig. 3). The percentage anisotropy in compressibility and shear are defined as [18] $A_B = (B_V - B_R)/(B_V + B_R)$, and $A_G = (G_V - G_R)/(G_V + G_R)$, respectively, where B and G are the bulk and shear modulus, and the subscripts V and R represent the Voigt and Reuss bounds. The elastic isotropy crystal has value equal to zero. The calculated results are collected in table 3. The slight value of A_B and A_G show that, Imma-carbon is almost isotropic in compressibility and shear. To illustrate the elastic anisotropy intuitively, a variation of Young's modulus with crystallographic direction is represented as three dimensional. The directional dependence of Young's modulus E for orthorhombic crystal is [18]:

$$\begin{aligned}\frac{1}{E} = {} & l_1^4 S_{11} + l_2^4 S_{22} + l_3^4 S_{33} + 2l_1^2 l_2^2 S_{12} + 2l_1^2 l_3^2 S_{13} \\ & + 2l_2^2 l_3^2 S_{23} + l_1^2 l_2^2 S_{66} + l_1^2 l_3^2 S_{55} + l_2^2 l_3^2 S_{44},\end{aligned} \tag{4}$$

where S_{ij} are the elastic compliance constants and l_1, l_2, and l_3 are the direction cosines. The calculated results are shown in fig. 3. The projection of Young's modulus along ab, ac, and bc planes are also shown in fig. 5. Figure 5(a) shows a small deviation from a spherical shape, this means Imma-carbon exhibit a small degree of anisotropy. With the pressure increasing, the degree of anisotropy increased,

Table 4: Hardness anisotropy of Imma-carbon (in GPa) by Li *et al.*'s model. The calculated results by other models presented by Chen *et al.* [24], Gao *et al.* [25], and Lyakhov *et al.* [26] are also listed for comparison.

Crystal	Method	[100]	[010]	[001]	[110]	[111]	H_v (Chen-Niu)	H_v (Gao-Tian)	H_v (Lyakhov-Oganov)
Imma-carbon[(a)]	GGA	83.8	84.3	83.7	83.4	83.6	79.6	72.8	84.9
	LDA	87.8	88.3	87.0	87.6	87.0	77.8	75.6	88.7
Diamond[(b)]		88.5			89.3	89.7	93.9	93.6	89.7
Bct-C_4[(c)]		90.1		88.8	89.0	88.0	71.3	77.1	87.7

[(a)] This work.
[(b)] Reference [21].
[(c)] The structure data are taken from ref. [22].

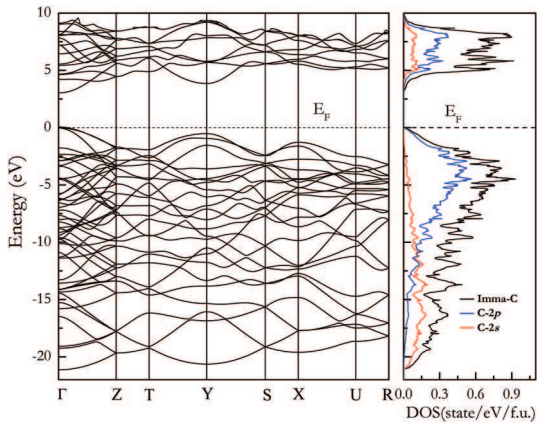

Fig. 6: (Colour on-line) Energy band structure and density of state of Imma-carbon at 0 GPa.

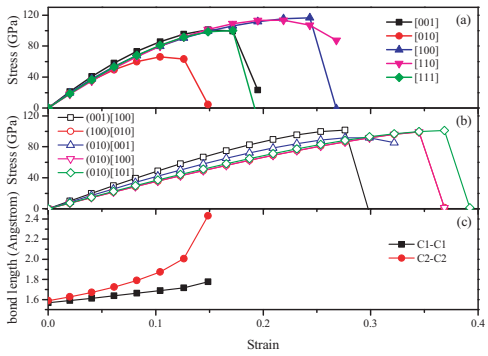

Fig. 7: (Colour on-line) Tensile strength (a) and shear strength (b) of Imma-carbon, and the C1-C1 and C2-C2 bond lengths as a function of tensile strain along the [010] direction (c).

as shown in figs. 5(b) and (d). Comparing figs. 5(b), (c), and (d), one can see that the increasing of the degree of anisotropy mainly occurred in the *ab* plane. The degree of anisotropy is almost the same in the *ac* plane when pressure increased.

To understand the mechanical properties of Imma-carbon on a fundamental level, the band structure, total and partial densities of states (DOS) were calculated at zero pressure, as shown in fig. 6. Clearly, it can be seen that Imma-carbon is a direct band gap semiconductor with 2.97 eV gap at Γ-point. Because density functional theory calculations usually lead to its underestimation, we recalculated the band gap by using HSE06 hybrid functional, and the obtained gap is 4.17 eV. From the partial DOS, it reveals that the peaks from −10 to −0 eV are mainly attributed to C-2*p* states with a small contribution from C-2*s*. The states from −20 to −10 eV mainly originated from C-2*p* and C-2*s* orbitals, and the partial DOS profiles for both C-2*p* and C-2*s* are very similar in the range of −20 to −10 eV, reflecting the significant hybridization between these two orbitals. This fact also shows a strong covalent interaction between C atoms. A similar case can be seen in the conduction band region of DOS.

In view of the large elastic moduli of Imma-carbon, the hardness calculations are of great interest. Previous studies have demonstrated that the ultimate hardness of a material may be assessed from its ideal strength, which also appears to correlate with the onset of dislocation formation in an ideal, defect-free crystal. Thus, the comprehensive analysis of the bonding nature and of ideal shear strength can provide a deeper insight into mechanical behaviour and hardness of materials. The calculations of ideal strengths for Imma-carbon were performed within GGA. For tensile deformation, the main high symmetry directions, including [001], [010], [100], [110], and [111], are considered as the tension directions. The calculated stress-strain curves for tensile strength are shown in fig. 7(a). One can see that the largest ideal tensile strength (116.6 GPa) appears in the [100] direction. The smallest value of 66.0 GPa is the tensile strength along the [010] direction, which means under tensile loadings, Imma-carbon would first cleave in the (010) plane. The shear strength was then calculated by applying [001], [100], and [101] shear deformations in the (010) easy cleavage plane perpendicular to the weakest tensile direction, as shown in fig. 7(b). The shear strength in the (001)[100] and (100)[010] directions are also shown in fig. 7(b) for comparison. The lowest peak shear stress occurs in the (010)[001]

direction with 91.7 GPa, which larger than the lowest tensile strength. This means the failure mode in Imma-carbon is dominated by the tensile type with 66.0 GPa, which is slightly larger than that of c-BN (55.3 GPa) [19] and w-BN (62 GPa) [20]. To understand the origin of deformation mechanism in this direction, the variations of bond lengths as a function of applied strain under the [010] direction were plotted in fig. 7(c). At the equilibrium state as presented in fig. 1(a), there are two types of C-C bonds along the [010] direction, one is C1-C1 bond with the bond length of 1.5679 Å and the other is C2-C2 bond with the bond length of 1.5894 Å. When tensile strain is applied along the [010] direction, one can imagine that the bond length of these two types of bonds will be elongated. Then the failure mode would correspond to the break of C1-C1 or C2-C2 bond along the [010] direction. To ensure this point, we have checked the bond length of C1-C1 and C2-C2 bonds along the [010] direction with applying tensile strain (fig. 7(c)). From fig. 7(c), the bond length of C2-C2 increases more rapidly due to its larger bond length compared to that of C1-C1 bond. Finally, C2-C2 bonds are broken at the critical tensile strain of 0.0612, which limits its achievable strengths. Subsequently, C1-C1 bonds are broken at the strain of 0.1487, resulting in the formation of zigzag layered graphite-like structure with six-carbon rings in Imma-carbon. Using an empirical model for the hardness of materials proposed in ref. [21], the hardness along the [100], [010], [001], [110], and [111] directions of Imma-carbon is calculated within GGA and LDA, as listed in table 4. The results show that the hardness along the [010] direction is slightly larger than the other directions. Since the difference of hardness along various directions is slight, we can regard Imma-carbon as an isotropy hardness material at equilibrium state. As mentioned above, the hardness of Imma-carbon is the largest along the [010] direction, whereas the ideal tensile strength is the lowest along this direction. The same phenomenon also occurred in the [111] direction of diamond and the [100] direction of Bct-C_4 (see table 4 and refs. [22,23]). For comparison, we calculated the hardness using various models [24–26], the calculated results are in the range of 72.8–84.9 GPa.

Conclusions. – In summary, we have carried out first-principles calculations on structural and mechanical properties as well as ideal strengths for recently proposed Imma-carbon. The calculated equilibrium lattice parameters are consistent with previous theoretical results. Phonon dispersion and elastic constants calculations have demonstrated that Imma-carbon is dynamically and mechanically stable at ambient condition. The anisotropy of elastic properties and hardness show that Imma-carbon is nearly mechanical isotropy at ambient condition. The substantially large tensile and shear strength of Imma-carbon indicates that it can be intrinsically superhard. Detailed analyses of the deformed atomic structures under tensile strain reveal that the lattice instability of Imma-carbon is due to the C-C bond break along the [010] direction.

* * *

This work was supported by the National Natural Science Foundation of China (Grant No. 11204007), the Natural Science Basic Research plan in Shaanxi Province of China (Grant No. 2012JQ1005, 2013JQ1007), Education Committee Natural Science Foundation in Shaanxi Province of China (Grant No. 2013JK0638), and the Fundamental Research Funds for the Central Universities.

REFERENCES

[1] Boulfelfel S. E., Oganov A. R. and Leoni S., *Sci. Rep.*, **2** (2012) 471.
[2] Wang Y., Panzik J. E., Kiefer B. and Lee K. K. M., *Sci. Rep.*, **2** (2012) 520.
[3] Li Q., Ma Y., Oganov A. R., Wang H. and Xu Y., *Phys. Rev. Lett.*, **102** (2009) 175506.
[4] Tian F., Dong X., Zhao Z., He J. and Wang H., *J. Phys.: Condens. Matter*, **24** (2012) 165504.
[5] Zhu Q., Zeng Q. and Oganov A., *Phys. Rev. B*, **85** (2012) 201407(R).
[6] He C., Sun L., Zhang C. and Zhong J., *Phys. Chem. Chem. Phys.*, **15** (2013) 680.
[7] Li D., Bao K., Tian F., Zeng Z., He Z., Liu B. and Cui T., *Phys. Chem. Chem. Phys.*, **14** (2012) 4347.
[8] Niu H., Chen Q., Wang S., Li D., Mao W. L. and Li Y., *Phys. Rev. Lett.*, **108** (2012) 135501.
[9] Wang J. T., Chen C. and Kawazoe Y., *Phys. Rev. Lett.*, **106** (2011) 075501.
[10] Umemoto K., Wentzcovitch R. M., Saito S. and Miyake T., *Phys. Rev. Lett.*, **104** (2010) 125504.
[11] Zhang X., Wang Y., Lv J., Zhu C. and Li Q., *J. Chem. Phys.*, **138** (2013) 114101.
[12] Perdew J. P., Burke K. and Ernzerhof M., *Phys. Rev. Lett.*, **77** (1996) 3865.
[13] Ceperley D. M. and Alder B. J., *Phys. Rev. Lett.*, **45** (1980) 566.
[14] Kresse G. and Joubert D., *Phys. Rev. B*, **59** (1999) 1758.
[15] Hill R., *Proc. Phys. Soc. A*, **65** (1952) 349.
[16] Birch F., *Phys. Rev.*, **71** (1947) 809.
[17] Zhang M., Liu H., Du Y., Zhang X., Wang Y. and Li Q., *Phys. Chem. Chem. Phys.*, **15** (2013) 14120.
[18] Ravindran P., Fast L., Korzhavyi P. A. and Johnsson B., *J. Appl. Phys.*, **84** (1998) 4891.
[19] Zhang R. F. and Veprek S., *Phys. Rev. B*, **80** (2009) 233401.
[20] Zhang R., Veprek S. and Argon A. R., *Phys. Rev. B*, **77** (2008) 172103.
[21] Li K., Yang P. and Xue D., *Acta Mater.*, **60** (2012) 35.
[22] Xu Y., Gao F. and Hao X., *Phys. Status Solidi RRL*, **4** (2010) 200.
[23] Telling R. H., Pickard C. J., Payne M. C. and Field J. E., *Phys. Rev. Lett.*, **84** (2000) 5160.
[24] Chen X. Q., Niu H., Li D. and Li Y., *Intermetallics*, **19** (2011) 1275.
[25] Gao F., He J., Wu E., Liu S., Yu D., Li D., Zhang S. and Tian Y., *Phys. Rev. Lett.*, **91** (2003) 015502.
[26] Lyakhov A. O. and Oganov A. R., *Phys. Rev. B*, **84** (2011) 092103.